



**HAL**  
open science

# Predicting short-period spectral ordinates of hybrid ground shaking prediction tools: a comparative benchmark

F Gatti, Fernando Lopez-caballero

► **To cite this version:**

F Gatti, Fernando Lopez-caballero. Predicting short-period spectral ordinates of hybrid ground shaking prediction tools: a comparative benchmark. 13th International Conference on Applications of Statistics and Probability in Civil Engineering(ICASP13), May 2019, Seoul, South Korea. hal-02142978

**HAL Id: hal-02142978**

**<https://hal.science/hal-02142978>**

Submitted on 22 Nov 2021

**HAL** is a multi-disciplinary open access archive for the deposit and dissemination of scientific research documents, whether they are published or not. The documents may come from teaching and research institutions in France or abroad, or from public or private research centers.

L'archive ouverte pluridisciplinaire **HAL**, est destinée au dépôt et à la diffusion de documents scientifiques de niveau recherche, publiés ou non, émanant des établissements d'enseignement et de recherche français ou étrangers, des laboratoires publics ou privés.

# Predicting short-period spectral ordinates of hybrid ground shaking prediction tools: a comparative benchmark

Filippo Gatti

*Research Engineer, Lab.MSSMat CNRS 8579, CentraleSupélec, Univ. Paris Saclay*

Fernando Lopez-Caballero

*Assistant Professor, Lab.MSSMat CNRS 8579, CentraleSupélec, Univ. Paris Saclay*

**ABSTRACT:** In this paper, a comparative perspective is provided on the efficiency and drawback of hybrid techniques to produce broad-band (BB) seismic time-histories, based on physics-based numerical simulations. The recently developed ANN2BB technique (Paolucci et al., 2018) is put under focus: it exploits Artificial Neural Networks (ANN) to predict short-period response spectra, feeding the algorithm with the low frequency outcome numerical simulations and producing hybrid broad-band (0-30 Hz) time-histories. The robustness of the methodology is argued by inputting correlated (from observations) and uncorrelated long-period spectral ordinates into the ANN predictive tool to draw an uncertainty map of possible predictions and test its sensitivity in relationship with the a priori accuracy numerical simulations.

## 1. INTRODUCTION

In the last decades, the impressive technological development in high-performance parallel super-computing endowed the engineering-seismological community with powerful computational tools to deterministically reproduce 3-D regional scale earthquake scenarios and render complex seismic wave-fields (Ichimura et al., 2016; Fu et al., 2017). Those tools incarnate the evergreen dream of controlling the whole multi-scale earthquake phenomenon in a deluxe virtual laboratory which includes the active faults, the complex buried and surface topography, the non-linear heterogeneous rheology of the Earth's crust and of the soil deposits, the structural components (Gatti et al., 2017, 2018a,c,b; Chabot et al., 2018). However, except very few examples, high-fidelity forward physics-based simulations of the source-to-site seismic wave-propagation are still limited, at present, to rather long wave-lengths, below 10 Hz. This impossibility of shattering this ceiling and produce re-

liable broad-band (0-30 Hz) earthquake scenarios is not solely inherited from its actual technological infeasibility (computational burden is still practically hard to treat, although promising advancements have started in this sense, exploiting hexaflop architectures) but resides mostly in the lack of data to constraint deterministic models at high frequency. As a matter of fact, Physics-Based Simulations (PBSs) embody a rigorous seismic-wave propagation model (i.e., including source, path, and site effects), which is however reliable only in the long-period range (typically above 0.20-0.25 s), owing to the limitations posed both by computational constraints and by insufficient knowledge of the medium at short wavelengths. That being the case, alternatives strategies to represent the high-frequency part of the observed earthquake ground shaking have been crafted. One of the most promising ones, based on hybridization technique firstly proposed by Graves and Pitarka (2004), was recently proposed by Paolucci et al. (2018). The authors proposed a novel approach, called ANN2BB, to generate broad-band (BB) ground

motions, which couples the results of PBS for a specific earthquake ground-motion scenario with the predictions of an Artificial Neural Network (ANN), overcoming some of the main issues of hybrid modeling. The basic steps of the procedure can be summarized as follows: (1) the ANN is trained on a strong-motion dataset, to correlate short-period ( $T \leq T^*$ ) spectral ordinates with the long-period ones ( $T \geq T^*$ ), being  $T^*$  the threshold period beyond which the results of the PBS are supposed to be accurate; (2) the trained ANN is used to obtain the short-period spectral ordinates of the physics-based earthquake ground motion for periods below  $T^*$  (Figure ??); and (3) the PBS long-period time histories are enriched at high frequencies with an iterative spectral matching approach, until the response spectrum matches the short-period part obtained by the ANN. Recently Gatti et al. (2018b) exploited high-fidelity numerical simulations and ANN2BB to reproduce the seismic response of a nuclear reactor building at the Japanese nuclear site of Kashiwazaki-Kariwa. They employed the synthetic wave-forms generated by a high-fidelity numerical simulations to feed the ANN2BB workchain and produce BB synthetics to be used as input for the Soil-Structure Interaction analysis at the reactor building scale.

In this paper, a deeper investigation on the ANN2BB procedure is performed, aiming at explaining its predictive power and highlight eventual drawbacks. This analysis is carried out by means of standard sensitivity analysis, such as the Sobol indices, whose response puts ANN2BB into critical perspective, so to improve it in future works.

## 2. ANN2BB OUTLINE

### 2.1. Methodology

Owing to the limitations posed both by computational constraints and by insufficient knowledge of the medium at short wavelengths (i.e. the mesh size and the poor description of the fault mechanism and geology) physics-based simulations of the earthquake mechanism are regarded as reliable in the long-period (LP) range (typically for natural periods  $T > T^*=0.75-1$  s). Figure 1a shows a typical pseudo-acceleration response spectra  $S_a$  for PBS (blue line), with evident numerical disper-

sion at SP, compared to the stochastic/empirical  $S_a$  prediction (STO/EMP, red line, obtained by several alternative approaches, as for instance Sabetta and Pugliese (1996)).

Hybrid broad-band wave-form (black-dashed  $S_a$  spectrum), obtained for instance with the method proposed by Graves and Pitarka (2004), are directly exploitable as spectrum-compatible input motions for seismic design of aboveground structures. Although realistic at the single station, the STO/EMP prediction fails in rendering the spatial distribution of the High Frequency (HF) Intensity Measures (IMs, i.e. PGA). To cope with these limitation, Paolucci et al. (2018) proposed to make use of ANN, trained on a set of strong motion records, to predict the response spectral ordinates at short periods (SP), using as input the LP ones obtained by the PBS (blue  $S_a$  spectrum in Figure 1a), and, then, to enrich the PBS time-histories by scaling iteratively their Fourier spectrum the ANN target spectrum (in small axes in Figure 1b). Further technical details on this so called ANN2BB procedure are outlined in Paolucci et al. (2018).

Compared to a standard hybrid approach, ANN2BB yields realistic waveforms, both in time and frequency domains, as well as it renders maps of short-period peak values of ground motion which reproduce more closely the coupling of source-related and site-related features of earthquake ground motion. The approach is suitable to portray in a realistic way the spatial correlation features of the peak values of ground motion although it is not suitable yet to obtain sets of waveforms with realistic spatial coherency features at high frequency. Another issue to be deemed is the choice of the training dataset to be fairly representative of the earthquake process at hand (Paolucci et al., 2018).

In this study, the teaching dataset is represented by the SIMBAD database (Smerzini et al., 2014), consisting of  $N_{db}=501$  three components high-quality accelerograms recorded world-wide, spanning a range of  $M_W$  from 5 to 7.4 and epicentral distances less than 40 km. Two ANNs were iteratively trained upon this training set (refer to Paolucci et al. (2018) for details on the training process and gen-

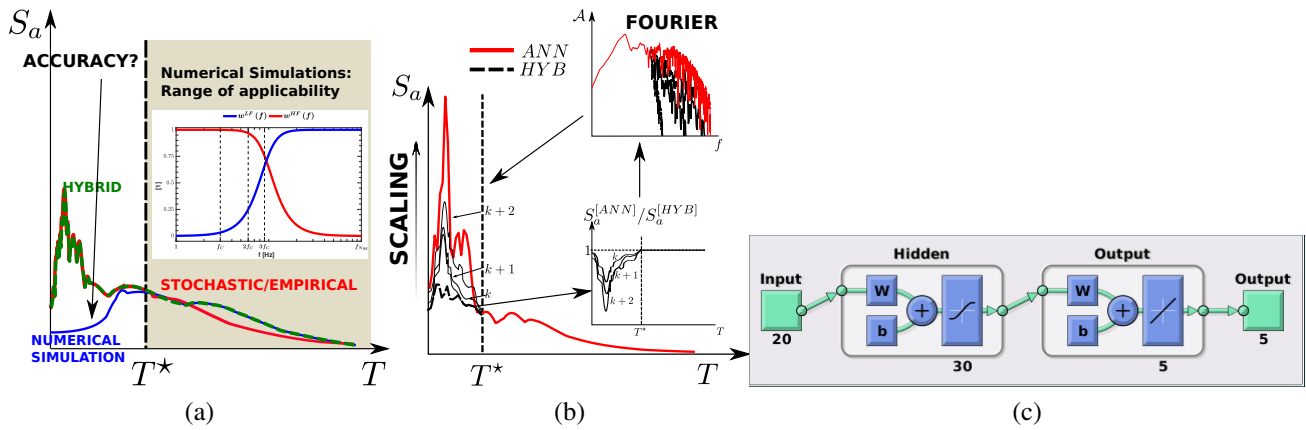


Figure 1: (a)  $S_a$  response spectra obtained by wave-propagation simulation (PBS, blue), by stochastic/empirical predictive methods (STO/EMP, orange) and by classical hybridization methods of the two (HYB, black dashed) (see Graves and Pitarka (2004); Smerzini and Villani (2012)). (b)  $S_a$  spectral matching iterative procedure: the red target spectrum is obtained by ANN prediction upon PBS LP values at long periods. The SP part is iteratively scaled, starting from the HYB trial, by computing the ratio  $S_a^{(ANN)}/S_a^{(HYB)}$  at each iteration and applying it as a corrective scaling factor in the Fourier's domain. (c) Scheme of the ANN architecture employed in this study.

eralization features), one referring to the geometric mean of the horizontal components and one to the vertical one. In our case, the neural network is designed as a feed-forward two-layers Perceptron (Bishop, 1995; Bishop and Roach, 1992), featured by  $N_n^h=30$  sigmoid hidden neurons and a linear output. The number of nodes in the input layer  $N_n^i$  equals the number of input variables  $N_{Sa}^{LP}$ , whereas the number of nodes in the output layer  $N_n^o$  equals the number of target values  $N_{Sa}^{SP}$ . The ANNs were trained by exploiting the Levenberg-Marquardt algorithm (Levenberg, 1944; Marquardt, 1963) to perform back-propagation of the error and adjust the weights<sup>1</sup> (see Paolucci et al. (2018) for further details and Figure 1c).

In the training phase, it is natural to investigate the ANN performance at hand on a test database, for instance on the  $S_a$  profiles obtained from recordings not belonging to the teaching dataset.

To prove ANN2BB efficiency, we tested it on the synthetic time-histories obtained by Gatti et al. (2018a) in the surroundings of the Kashiwazaki-

Kariwa nuclear power plant, in their numerical simulation<sup>2</sup> of one of the aftershock (AS1) of the 2007 Mw6.8 Niigata earthquake. The earthquake ground motion simulations performed in Gatti et al. (2018a) are reliable up to 5 Hz. The *jump* from 5 to 30 Hz is performed by applying the ANN2BB procedure, upon training with corner period  $T^*=0.75$  s. Figures 2 portrays the site response (in terms of  $S_a$ , with 5% damping) at stations SG1 (Service Hall, G.L. -2.7 m, Figures 2a) and for 1G1 (Unit 1, G.L. 0 m, 2b) respectively. It is evident that feeding the ANN2BB procedure with the seismic wave-motion obtained by a refined site-specific numerical analysis (including the folding structure) improves the overall broad-band prediction of the outcropping wave-motion. Figure 3 shows the ANN2BB time-histories (in a 0.1-30 Hz frequency range) which were exploited as synthetic input wave-motion for the structural model of the Unit 7 reactor building. The improved outcome of the broad-band synthetics obtained by ANN2BB confirms somehow the fact that the predictive methodology inherits the information concerning spatial distribution of the earthquake ground motion and it propagates it to shorter periods. This is an interesting phe-

<sup>1</sup>At this stage, the neural network fitting tools (nftool) implemented in Matlab is used. MATLAB is available at <https://fr.mathworks.com/solutions/deep-learning.html> (last accessed March 2018).

<sup>2</sup>performed by means of SEM

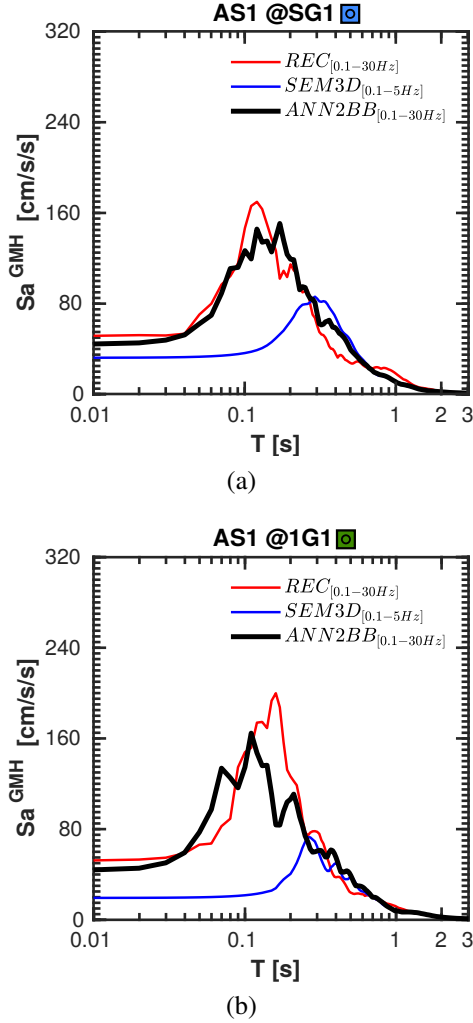


Figure 2: Sa spectra after ANN2BB application on the SEM3D analysis performed for AS1, at the Service Hall of the KKNPP site: (a) SGI, G.L. -250 m, (b) 1G1, G.L. 0 m respectively. REC (red), SEM3D (blue) and ANN2BB (black) are the recorded, simulated and enriched Sa spectra respectively. REC and ANN2BB signals were filtered between 0.1-30 Hz, SEM3D synthetics between 0.1-5 Hz.

nomenon, since it proves the exceptional capability of neural networks to recognize the input pattern and predict the outcome based on the experience gained during the training phase. Even when SEM3D analyses provided poor fit to the records (probably due to the effect of shallow geotechnical layers, not considered in the 3-D numerical analyses at regional scale), the ANN2BB provides more reasonable spectral ordinates, recommending its utilization to generate realistic broad-band synthet-

ics. It has to be noted again that the ANN employed at this stage were trained upon the SIMBAD database Smerzini et al. (2014), containing high-quality recordings observed for earthquakes in a magnitude range  $M_W 5.0-7.5$ . Despite the fact that AS1 has a magnitude  $M_W 4.4$ , the satisfactory results obtained ensure somehow the reliability of the ANN predictive capabilities.

It is reasonable to disregard the non-linear site-effects occurred during the main shock, since a small aftershocks were solely considered.

### 3. SENSITIVITY ANALYSIS ON ANN2BB

#### 3.1. Influence of the correlation Sa correlation structure at LP

To assess the sensitivity of the ANN2BB prediction with respect to the input spectral ordinates  $Sa_i^{SP} \in \mathbb{R}^+$ , a multi-variate log-normal random fluctuation was added to it:

$$\log(\mathbf{Sa}^{SP}) = \log(\boldsymbol{\mu}_{\mathbf{Sa}^{SP}}) + \mathbf{U}\mathcal{N}(0, \text{diag}[\boldsymbol{\Sigma}]) \quad (1)$$

where  $\boldsymbol{\mu}_{\mathbf{Sa}^{SP}}$  represents the random input vector of spectral ordinates at long periods,  $\boldsymbol{\Sigma}$  is the correlation matrix reported in Jayaram et al. (2011),  $\mathbf{U}$  its eigenvector and  $\mathcal{N}$  a random vector of  $N_{Sa}^{LP}$  i.i.d. normal distributed random variables. Figure ?? shows the outcome of the ANN2BB procedure when feeding it with uncorrelated (Figure 4a) and correlated (Figure 4b) spectral ordinates at long period. This first sensitivity analysis shows ANN2BB capability of recognizing the hidden patterns characterizing the input dataset. Those features are inherited by the prediction at short period: uncorrelated input values provide larger uncertainty on the output values.

#### 3.2. Sobol sensitivity indices

We further tested the sensitivity of the ANN2BB method by employing the global sensitivity analysis, known as Sobol's method. The latter decomposes the variance of the output vector ( $\mathbf{Y} = \mathbf{Sa}^{SP} \in \mathbb{R}^{N_{Sa}^{SP}+}$ ) of the model or system into fractions which can be attributed to inputs or sets of inputs ( $\mathbf{x} = \mathbf{Sa}^{LP} \in \mathbb{R}^{N_{Sa}^{LP}+}$ ). As a matter of fact, any ANN can be viewed a complex imbrication of non-linear regressions which expresses the output as a continuous function  $\mathbf{f} : \mathbb{R}^{N_{Sa}^{LP}+} \rightarrow \mathbb{R}^{N_{Sa}^{SP}+}$

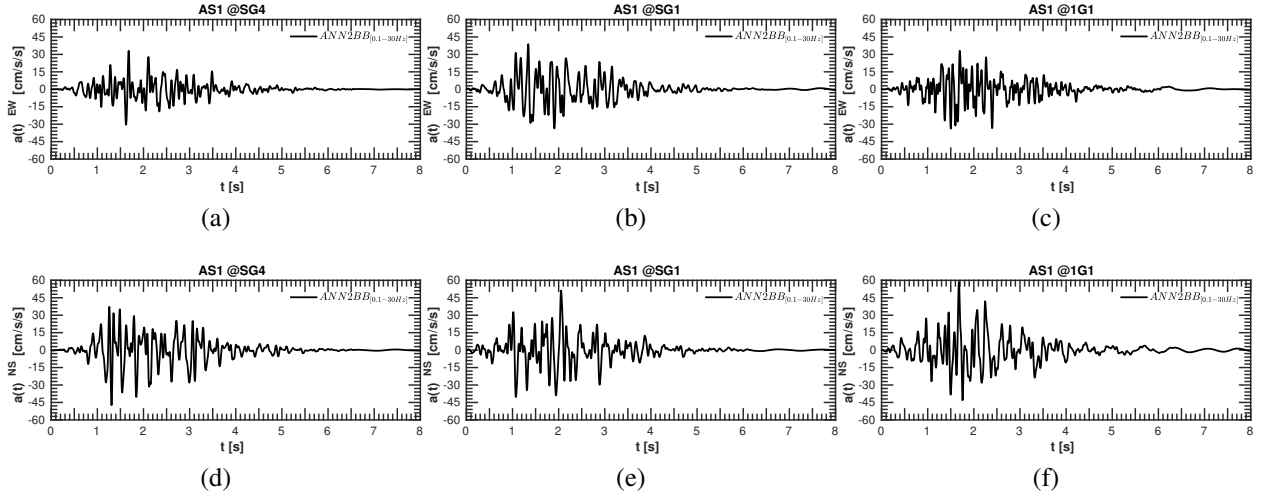


Figure 3: Acceleration time histories (EW-NS directions, in  $\text{cm/s}^2$ ) after ANN2BB application on the SEM3D analysis performed for AS1, at the Service Hall of the KKNPP site: (a-d) SG4, Service Hall, G.L. -250 m; (b-e) SG1, Service Hall, G.L. 0 m; (c-f) 1G1, Unit 1, G.L. 0 m. Synthetics were filtered between 0.1-30 Hz.

of the input:  $\mathbf{Y} = \mathbf{f}(\mathbf{x})$ . However,  $\mathbf{f}$  rarely has explicit form (depending on the complexity and the depth of the ANN). Moreover, the input random vector  $\mathbf{x}$  has a auto-covariance structure that has been stated by performing statistics on strong motion databases, but that is very difficult to be unraveled by analytical derivations from an underlying physical model: the values of  $Sa$  are the result of a non-linear filter on the Single-Degree-Of-Freedom equation (SDOF), by taking the maximum absolute displacement value for each natural period  $T$  and multiplying it by  $(\frac{2\pi}{T})^2$ . Therefore, without loss of generality, the input random vector is considered composed by i.i.d. (independent identically distributed) variables  $x_i$ . For the sake of simplicity, a uniform distribution is assumed:  $u_i \sim \mathcal{U}[\mu_{x_i}(1 - CV); \mu_{x_i}(1 + CV)]$  with Coefficient of Variation  $CV = 0.1$  and  $\mu_{x_i}$  the average value, taken as the  $Sa_i^{LP}$  obtained by numerical simulation. This incurs no loss of generality because any input space  $\mathcal{X}$  can be transformed onto this unit hypercube  $[0; 1]^{N_{Sa}^{LP}}$ , though the application of the cumulative distribution function  $\mathcal{F}$ .

Sobol method consists into approximate  $\mathbf{f}(\mathbf{x})$  by a

sum of *orthogonal* functions:

$$\mathbf{Y} = \mathbf{f}_0 + \sum_i^d \mathbf{f}_i(x_i) + \sum_{i < j}^d \mathbf{f}_{ij}(x_i; x_j) + \dots + \mathbf{f}_{1, \dots, i, \dots, j, d}(\mathbf{x}) \quad (2)$$

with  $d = N_{Sa}^{LP}$  and  $x_i = Sa_i^{LP}$ . A condition of this decomposition is that:

$$\int_0^1 \mathbf{f}_{i_1, i_2, \dots, i_s}(X_{i_1}, X_{i_2}, \dots, X_{i_s}) dX_k = 0, \forall k = i_1, i_2, \dots, i_s \quad (3)$$

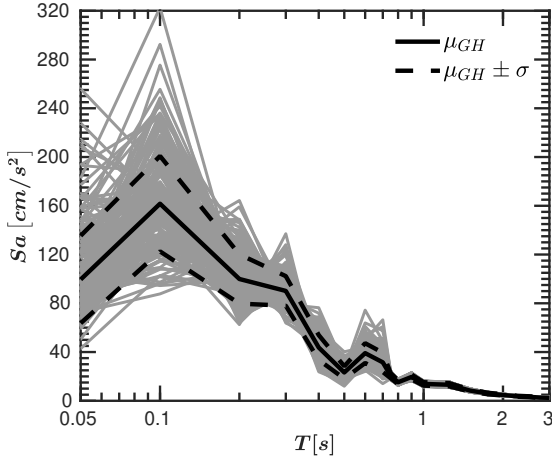
which expresses the *orthogonality* of the basis function used for the decomposition (in stochastic sense). The result relies on the Theorem of the Law of Total Variance, which states that:

$$\text{Var}[Y] = \text{Var}[\mathbb{E}[Y|X]] + \mathbb{E}[\text{Var}[Y|X]] \quad (4)$$

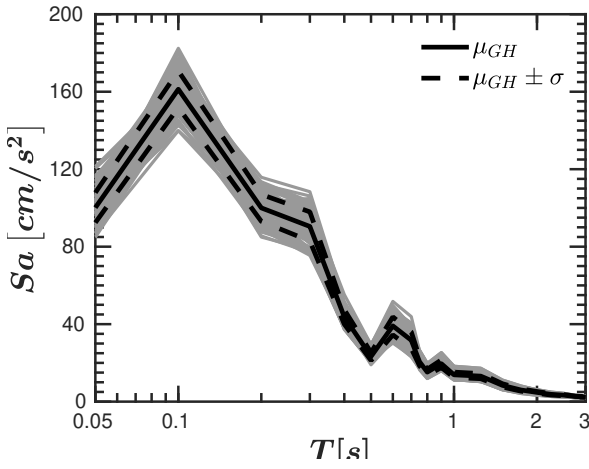
for any two random variables  $Y$  and  $X$ . The latter result extends to stochastic dynamic systems as:

$$\begin{aligned} \text{Var}[Y(t)] &= \text{Var}[\mathbb{E}[Y(t)|H_{1,t}]] + \\ &\sum_{j=2}^{r-1} \mathbb{E}[\text{Var}[\mathbb{E}[(Y|\{H_{k,t}\}_{k=2}^j) | \{H_{k,t}\}_{k=1}^{j-1}]]] + \\ &\mathbb{E}[\text{Var}[Y(t) | \{H_{k,t}\}_{k=1}^{r-1}]] \end{aligned} \quad (5)$$

where  $H_{i,t}$  are the natural filtration associated to the stochastic process  $Y$ . Note that this approach examines scalar model outputs, but multiple outputs



(a)



(b)

Figure 4: Influence of the auto-correlation structure on the predicted values of ANN2BB at short period. (a) ANN2BB prediction obtained feeding it with sets of uncorrelated spectral ordinates at long period. (b) ANN2BB outcome feeding it with sets of correlated spectral ordinates at long period.

can be analysed by multiple independent sensitivity analyses. Owing to Equation (5), given the orthogonality condition (3), the functions  $f_{i,j,\dots}$  can be identified as:

$$\begin{aligned} \mathbf{f}_0 &= \mathbb{E}[\mathbf{Y}], \\ \mathbf{f}_i(x_i) &= \mathbb{E}[\mathbf{Y}|x_i] - \mathbf{f}_0, \\ \mathbf{f}_{i,j}(x_i, x_j) &= \mathbb{E}[\mathbf{Y}|x_i, x_j] - \mathbf{f}_i(x_i) - \mathbf{f}_j(x_j) - \mathbf{f}_0, \\ &\dots \end{aligned}$$

Moreover, the variance of the output can be expressed as:

$$\begin{aligned} \text{Var}[\mathbf{Y}] &= \sum_{i=1}^d \text{Var}[\mathbf{f}_i(x_i)] + \sum_{i \neq j}^d \text{Var}[\mathbf{f}_{i,j}(x_i, x_j)] + \\ &\dots \\ &+ \text{Var}[\mathbf{f}_{1,2,\dots,i,\dots,j,\dots,d}(\mathbf{x})] \end{aligned} \quad (7)$$

In this analysis, solely the first order Sobol indices were analyzed, which read (for the  $i^{\text{th}}$  output  $y_i$ ):

$$S_{i,j} = \frac{\text{Var}[\mathbb{E}[y_i|x_j] - \mathbb{E}[y_i]]}{\text{Var}[y_i]} \quad (8)$$

In this analysis, the trajectories to explore the multivariate distributions  $y_i[\mathbf{x}]$  were obtained by quasi-Monte Carlo (qMC) method: Figure 5 shows the obtained results (in terms of  $Sa$ ) for 2000 simulations. In Figure 6, the Sobol indices corresponding to the qMC simulations depicted in Figure 5 are reported: the sensitivity of the  $n^{\text{th}}$  output variable  $Sa^{SP}[T_n]$  is pictured by the corresponding Sobol indices at each  $m^{\text{th}}$  input variable  $Sa^{LP}[T_m]$ . The outcome of this sensitivity analysis outlines a few remarkable features of the ANN2BB procedure.  $Sa^{SP}$  values at very short-period ( $T < 0.2\text{s}$ ) are equally sensitive to the ensemble of  $Sa^{LP}$  values. For a range of natural periods  $T \approx 0.2 - 0.3\text{ s}$ , the ANN2BB prediction is mostly affected by the values of the long-period spectral ordinates closed to the corner period ( $T \in [0.75 - 1]\text{s}$ ). A major influence of the input spectral ordinates  $Sa^{LP}[T]$  for  $T \in [1.25 - 2]\text{s}$  is highlighted when considering  $Sa^{SP}$  values corresponding to  $T > 0.5\text{ s}$ . An equal and low sensitivity is shown for input spectral ordinates  $Sa^{LP}[T] > 2\text{ s}$  (with the exception of an unexpected peak at  $T > 4\text{s}$  for one of the stations considered).

#### 4. CONCLUSIONS

In this paper, a sensitivity analysis of the ANN2BB procedure proposed by Paolucci et al. (2018) is presented. The key idea is to enrich the synthetic wave motion rendered by regional scale earthquake simulations at high-frequency ( $f > 5\text{ Hz}$ ) by employing

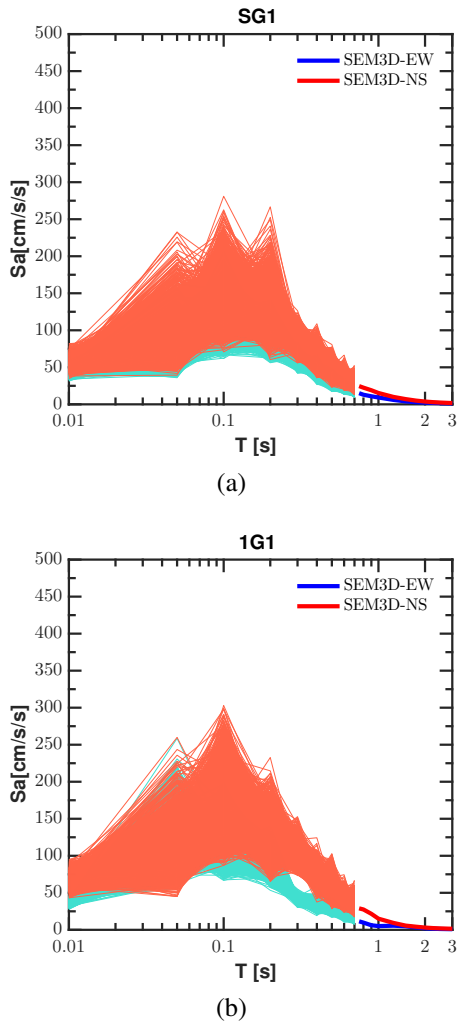


Figure 5:  $S_a$  values at SG1 (a) and 1G1 (b), produced by quasi-Monte Carlo simulation

a two-layers feed-forward Neural Network to predict the short-period part of the pseudo-spectral acceleration, given the long-period part provided by realistic synthetic wave-forms. In this study, Sobol indices were computed for the ANN2VBB framework, which carries the statistical information describing the variability of the pseudo-spectral prediction and its sensitivity to the spectral ordinates at longer periods. The outcome was obtained by polluting the input spectral ordinates (corresponding to  $T > 0.75$  s) with uniform random fluctuations, and running a quasi-Monte Carlo simulation to create the adapt sample space on which compute the statistical moments required. The Sobol indices highlighted the poor influence exerted by the spectral ordinates at  $T > 2$  s on the prediction of the

short-period portion. Given this insightful remark, a further improvement of the ANN2BB procedure is foreseen, reducing the number of input spectral ordinates, which resulted as redundant.

## 5. REFERENCES

- Bishop, C. (1995). *Neural Networks for Pattern Recognition*. Clarendon Press - Oxford.
- Bishop, C. and Roach, C. (1992). "Fast Curve Fitting using Neural Networks." *Review of Scientific Instruments*, 63(10).
- Chabot, S., Glinsky, N., Diego Mercerat, E., and Bonilla, L. F. (2018). "A High-Order Discontinuous Galerkin Method for Coupled Wave Propagation in 1D Elastoplastic Heterogeneous Media." *Journal of Theoretical and Computational Acoustics*, 26(03), 1850043.
- Fu, H., He, C., Chen, B., Yin, Z., Zhang, Z., Zhang, W., Zhang, T., Xue, W., Liu, W., Yin, W., Yang, G., and Chen, X. (2017). "18.9Pfpops Nonlinear Earthquake Simulation on Sunway TaihuLight: Enabling Depiction of 18-Hz and 8-meter Scenarios." *Proceedings of the International Conference for High Performance Computing, Networking, Storage and Analysis, SC '17*, New York, NY, USA, ACM, 2:1–2:12, <<http://doi.acm.org/10.1145/3126908.3126910>>.
- Gatti, F., Lopez-Caballero, F., Clouteau, D., and Paolucci, R. (2018a). "On the effect of the 3-D regional geology on the seismic design of critical structures: the case of the Kashiwazaki-Kariwa Nuclear Power Plant." *Geophysical Journal International*, 213(2), 1073–1092.
- Gatti, F., Paludo, L. D. C., Svay, A., Lopez-Caballero, F., Cottreau, R., and Clouteau, D. (2017). "Investigation of the earthquake ground motion coherence in heterogeneous non-linear soil deposits." *Procedia Engineering*, 199(Supplement C), 2354 – 2359 X International Conference on Structural Dynamics, EURODYN 2017.
- Gatti, F., Touhami, S., Lopez-Caballero, F., Paolucci, R., Clouteau, D., Alves Fernandes, V., Kham, M., and Voldoire, F. (2018b).

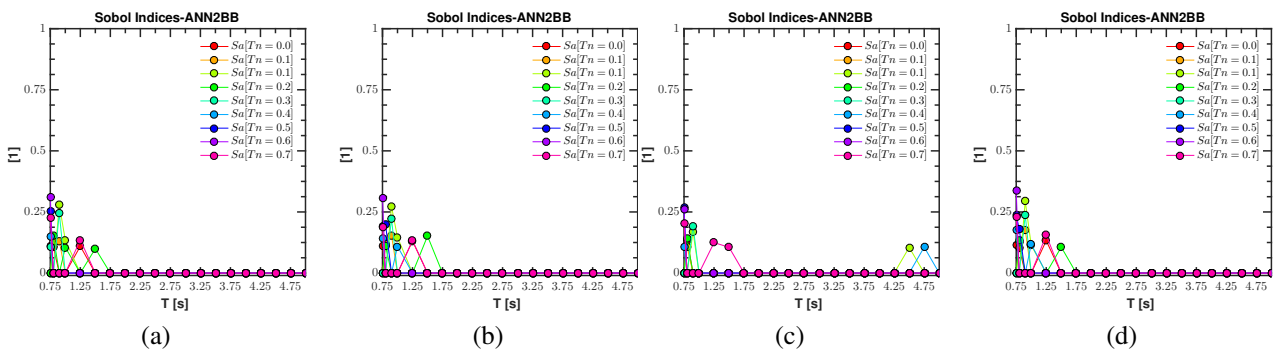


Figure 6: Sobol indices for two recording points SG1 and IG1: each point corresponds to the Sobol index of the input  $Sa^{LP}[T_i]$  onto the output indicated by the color. (a-b) Sobol indices for SG1, EW-NS directions. (c-d) Sobol indices for IG1, EW-NS directions.

“Broad-band 3-D earthquake simulation at nuclear site by an all-embracing source-to-structure approach.” *Soil Dynamics and Earthquake Engineering*, 115, 263–280.

Gatti, F., Touhami, S., Lopez-Caballero, F., and Pitilakis, D. (2018c). “3-D source-to-site numerical investigation on the earthquake ground motion coherency in heterogeneous soil deposits.” *NUMGE2018*.

Graves, R. W. and Pitarka, A. (2004). “Broadband time history simulation using a hybrid approach.” *13th World Conference on Earthquake Engineering, Vancouver, B.C., Canada*.

Ichimura, T., Agata, R., Hori, T., Hirahara, K., Hashimoto, C., Hori, M., and Fukahata, Y. (2016). “An elastic/viscoelastic finite element analysis method for crustal deformation using a 3-D island-scale high-fidelity model.” *Geophysical Journal International*, 206(1), 114–129.

Jayaram, N., Baker, J. W., Okano, H., Ishida, H., McCann Jr, M. W., and Mihara, Y. (2011). “Correlation of response spectral values in Japanese ground motions.” *Earthquake and Structures*, 2(4), 357–376.

Levenberg, K. (1944). “A method for the solution of certain non-linear problems in least squares.” *Quarterly of applied mathematics*, 2(2), 164–168.

Marquardt, D. W. (1963). “An algorithm for least-squares estimation of nonlinear parameters.” *Journal of the society for Industrial and Applied Mathematics*, 11(2), 431–441.

Paolucci, R., Gatti, F., Infantino, M., Ozcebe, A. G., Smerzini, C., and Stupazzini, M. (2018). “Broad-band ground motions from 3D physics-based numerical simulations using Artificial Neural Networks.” *Bulletin of the Seismological Society of America*, 108((3A)), 1272–1286.

Sabetta, F. and Pugliese, A. (1996). “Estimation of Response Spectra and Simulation of Nonstationary Earthquake Ground Motions.” *Bulletin of the Seismological Society of America*, 86(2), 337–352.

Smerzini, C., Galasso, C., Iervolino, I., and Paolucci, R. (2014). “Ground motion record selection based on broadband spectral compatibility.” *Earthquake Spectra*, 30(4), 1427–1448.

Smerzini, C. and Villani, M. (2012). “Broadband Numerical Simulations in Complex Near-Field Geological Configurations: The Case of the 2009 Mw 6.3 L’Aquila Earthquake.” *Bulletin of the Seismological Society of America*, 102(6), 2436–2451.